






ARTICLE

CCDC92 promotes podocyte injury by regulating PA28 α /ABCA1/cholesterol efflux axis in type 2 diabetic mice

Fu-wen Zuo¹, Zhi-yong Liu¹, Ming-wei Wang¹, Jun-yao Du¹, Peng-zhong Ding¹, Hao-ran Zhang¹, Wei Tang², Yu Sun¹, Xiao-jie Wang¹, Yan Zhang¹, Yu-sheng Xie¹, Ji-chao Wu¹, Min Liu¹, Zi-ying Wang¹ and Fan Yi^{1,3}

Podocyte lipotoxicity mediated by impaired cellular cholesterol efflux plays a crucial role in the development of diabetic kidney disease (DKD), and the identification of potential therapeutic targets that regulate podocyte cholesterol homeostasis has clinical significance. Coiled-coil domain containing 92 (CCDC92) is a novel molecule related to metabolic disorders and insulin resistance. However, whether the expression level of CCDC92 is changed in kidney parenchymal cells and the role of CCDC92 in podocytes remain unclear. In this study, we found that *Ccdc92* was significantly induced in glomeruli from type 2 diabetic mice, especially in podocytes. Importantly, upregulation of *Ccdc92* in glomeruli was positively correlated with an increased urine albumin-to-creatinine ratio (UACR) and podocyte loss. Functionally, podocyte-specific deletion of *Ccdc92* attenuated proteinuria, glomerular expansion and podocyte injury in mice with DKD. We further demonstrated that *Ccdc92* contributed to lipid accumulation by inhibiting cholesterol efflux, finally promoting podocyte injury. Mechanistically, *Ccdc92* promoted the degradation of ABCA1 by regulating PA28 α -mediated proteasome activity and then reduced cholesterol efflux. Thus, our studies indicate that *Ccdc92* contributes to podocyte injury by regulating the PA28 α /ABCA1/cholesterol efflux axis in DKD.

Keywords: CCDC92; proteasome activity; podocytes; cholesterol efflux; diabetic kidney disease

Acta Pharmacologica Sinica (2024) 45:1019–1031; <https://doi.org/10.1038/s41401-023-01213-4>

INTRODUCTION

Diabetic kidney disease (DKD), a major complication of diabetes, has been considered as the leading cause of end-stage renal disease (ESRD) [1]. An increasing number of studies have suggested that dysregulation of lipid metabolism in the kidney is a major determinant of DKD [2]. Although accumulation of lipids occurs in podocytes, mesangial cells and proximal tubule epithelial cells, different renal parenchymal cells show different sensitivities to lipid accumulation in DKD [3]. Notably, podocytes are especially sensitive to lipotoxic injury, causing insulin resistance and cell death [3]. Lipid metabolism in podocytes is a dynamic process, including lipid synthesis, uptake, oxidation, lipolysis and efflux [4, 5]. Recent studies indicate that impaired cellular cholesterol efflux plays a crucial role in the pathogenesis of podocytes [6–8]. Improving cholesterol efflux attenuates podocyte injury in glomerular disease [6]. Therefore, the identification of potential therapeutic targets that alter podocyte cholesterol efflux is of importance in DKD.

Coiled-coil domain containing 92 (CCDC92), also known as Limkain Beta 2 and FLJ22471, has been reported to be associated with obesity, type 2 diabetes (T2D), and coronary artery disease [9–12]. A very recent study demonstrated that *Ccdc92* knockout reduced obesity and increased insulin sensitivity under high-fat diet (HFD) conditions. Through the generation of *Ccdc92* knockout mice, the researchers mainly addressed the importance of CCDC92

in adipocyte differentiation and inflammation-mediated insulin resistance [13], and their results suggested that CCDC92 may be a key factor in metabolic disorders. However, the roles and exact mechanisms of CCDC92 in lipid metabolism and related diseases, especially diabetic kidney disease, are still unclear.

In this study, we found that CCDC92 was induced in podocytes from type 2 diabetic mice. *Ccdc92* deficiency in podocytes reduced lipid accumulation by increasing cholesterol efflux. Mechanistically, *Ccdc92* promoted the degradation of ATP-binding cassette transporter 1 (ABCA1) by regulating PA28 α -mediated proteasome activity, finally leading to the inhibition of cholesterol efflux in podocytes. Our findings suggest that *Ccdc92* contributes to podocyte injury by regulating the PA28 α /ABCA1/cholesterol efflux axis in DKD.

MATERIALS AND METHODS

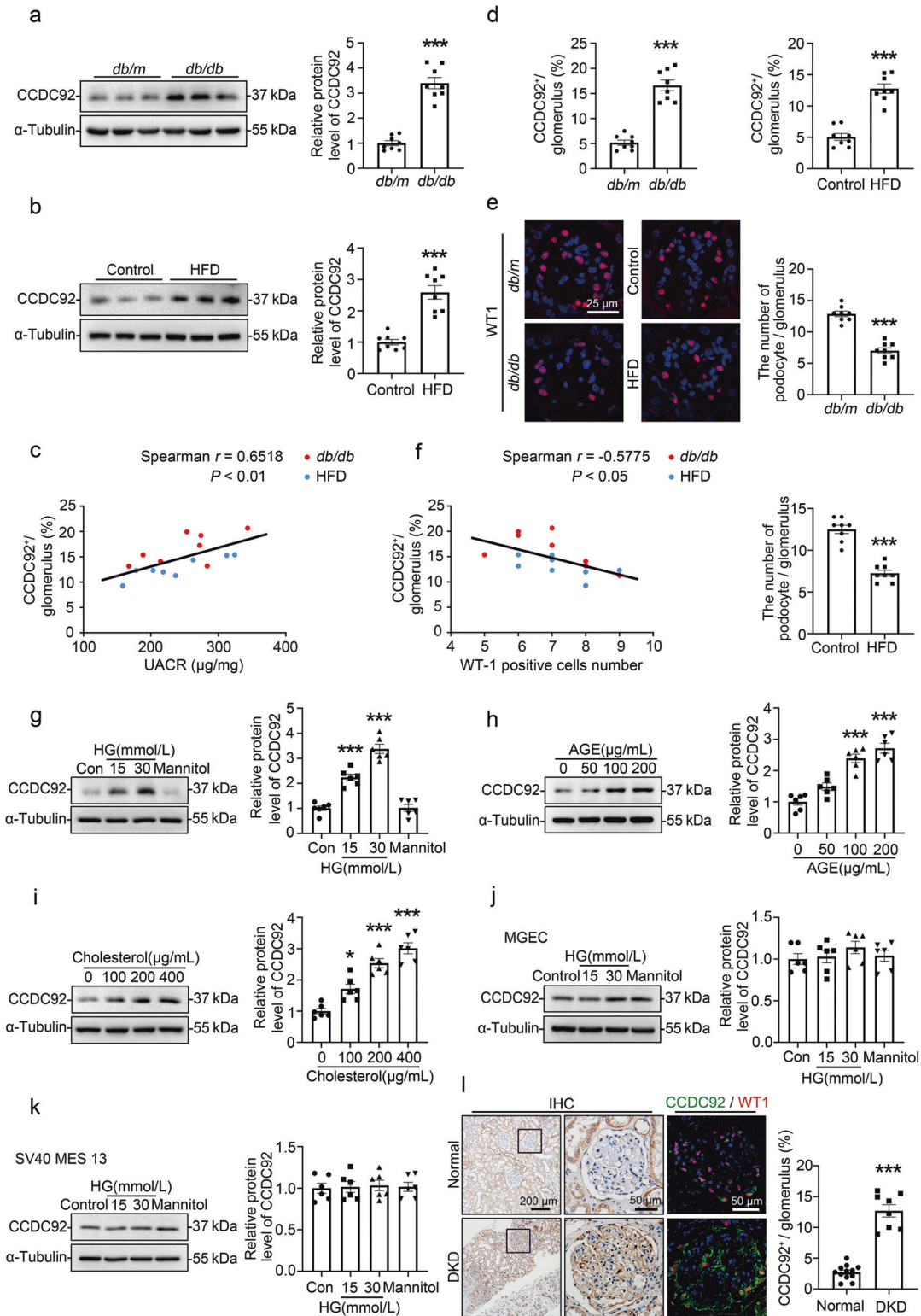
Details of the methods are provided in the supplementary complete materials and methods section.

Establishment of podocyte-specific *Ccdc92* knockout mice *Ccdc92*^{fl α /+} (*Ccdc92*^{fl/+}) mice (C57BL/6J) were provided by Shanghai Model Organisms Center, Inc. (Shanghai, China) and were crossed with mice expressing Cre recombinase (Cre) under the control of the podocin promoter (B6.Cg-Tg[NPHS2-cre]295Lbh/J;

¹Department of Pharmacology, School of Basic Medical Sciences, Shandong University, Jinan 250012, China; ²Department of Pathogenic Biology, School of Basic Medical Sciences, Shandong University, Jinan 250012, China and ³National Key Laboratory for Innovation and Transformation of Luobing Theory, Key Laboratory of Cardiovascular Remodeling and Function Research, Chinese Ministry of Education and Chinese Ministry of Health, Qilu Hospital, Shandong University, Jinan 250012, China
Correspondence: Min Liu (liuweimin@sdu.edu.cn) or Ziying Wang (wangziying@sdu.edu.cn) or Fan Yi (fanyi@sdu.edu.cn)

Received: 21 August 2023 Accepted: 7 December 2023

Published online: 16 January 2024



The Jackson Laboratory) to generate mice with podocyte-specific *Ccdc92* knockout mice (*Podocin-Cre/Ccdc92^{fl/fl}; Cre⁺/Ccdc92^{fl/fl}*).

Spontaneous type 2 diabetic *db/db* (BKS) mice Heterozygous BKS *db/m* mice (BKS.Cg-Dock7^m +/+Lepr^{db}/J, Stock No. 000642) and homozygous BKS *db/db* mice (B6.BKS(D)-Lepr^{db}/J, Stock No.000697) were purchased from The Jackson Laboratory.

Generation of podocyte-specific *Ccdc92* knockout mice with spontaneous type 2 diabetes

Mice with podocyte-specific *Ccdc92* deletion mice (*Cre⁺/Ccdc92^{fl/fl}*) were crossed with *db/+* mice to generate *db/+//Cre⁺/Ccdc92^{fl/+}* mice, which were crossed with *db/+//Cre⁺/Ccdc92^{fl/+}* mice to obtain *db/+//Cre⁺/Ccdc92^{fl/fl}* and *db/+//Cre⁺/Ccdc92^{fl/+}* mice. Then, *db/+//Cre⁺/Ccdc92^{fl/fl}* mice were crossed with *db/+//Cre⁺/Ccdc92^{fl/+}*

Fig. 1 Ccdc92 was involved in podocyte injury under diabetic kidney disease. **a** Representative Western blot gel documents and summarized data showing the relative protein levels of Ccdc92 in the cortex of kidney from *db/db* mice ($n = 8$ for each group). $***P < 0.001$ vs. control mice. **b** Representative Western blot gel documents and summarized data showing the relative protein levels of Ccdc92 in the cortex of kidney from HFD-induced diabetic mice ($n = 8$ for each group). $***P < 0.001$ vs. control mice. **c** Correlation between glomerular Ccdc92 expression and urine albumin to creatinine ratio (UACR) in all subjects ($n = 16$). **d** Statistical analyses of Ccdc92 in glomeruli from *db/db* and HFD induced diabetic mice detected by IHC ($n = 8$ for each group). $***P < 0.001$ vs. control mice. **e** Photomicrographs and quantifications showing the staining of Wilms' Tumor 1 (WT1, used as a podocyte marker) in the kidney from *db/db* or HFD induced diabetic mice ($n = 8$ for each group). $***P < 0.001$ vs. control mice. **f** Correlation between glomerular Ccdc92 expression and WT-1 in all animals ($n = 16$). **g** Representative Western blot gel documents and summarized data showing the relative protein levels of Ccdc92 in mouse podocytes treated with high glucose (HG, 15 or 30 mmol/L) for 24 h ($n = 6$ for each group). Mannitol was used as the osmotic pressure control for HG. $***P < 0.001$ vs. control. **h** Representative Western blot gel documents and summarized data showing the relative protein levels of Ccdc92 in podocytes treated with advanced glycation end-product (AGE, 50-200 $\mu\text{g}/\text{mL}$) for 24 h ($n = 6$ for each group). $***P < 0.001$ vs. control. **i** Representative Western blot gel documents and summarized data showing the relative protein levels of Ccdc92 in podocytes treated with cholesterol (100-400 $\mu\text{g}/\text{mL}$) for 24 h ($n = 6$ for each group). $*P < 0.05$, $***P < 0.001$ vs. control. **j** Representative Western blot gel documents and summarized data showing the relative protein levels of Ccdc92 in mouse glomerular endothelial cells (MGEC) treated with high glucose (HG, 15 or 30 mmol/L) for 24 h ($n = 6$ for each group). Mannitol was used as the osmotic pressure control for HG. **k** Representative Western blot gel documents and summarized data showing the relative protein levels of Ccdc92 in mouse mesangial cells (SV40 MES 13) treated with high glucose (HG, 15 or 30 mmol/L) for 24 h ($n = 6$ for each group). Mannitol was used as the osmotic pressure control for HG. **l** Representative immunohistochemistry (IHC) and immunofluorescence (IF) images and quantification of glomerular Ccdc92 expression (based on IHC) from normal subjects ($n = 12$) and patients with DKD ($n = 8$). Data are expressed as mean \pm SEM and n indicates the number of biologically independent experiments. Two-tailed Student's unpaired t test analysis (**a**, **b**, **d–e**), one-way ANOVA followed by Tukey's post-test (**g–k**), Spearman's correlations (**c**, **f**), Kruskal-Wallis test followed by Dunn's post-test (**l**).

mice to generate podocyte-specific *Ccdc92* knockout mice with spontaneous type 2 diabetes (*db/db/Cre⁺/Ccdc92^{fl/fl}*). In addition, *db/db/Cre⁺/Ccdc92^{fl/fl}* mice were used as controls.

Establishment of HFD-induced DKD in mice

Six-week-old male *Cre⁺/Ccdc92^{fl/fl}* mice and their littermate *Cre⁻/Ccdc92^{fl/fl}* mice were fed either a high-fat diet (HFD; 60 kcal% from fat, Research Diets, D12492) or a control diet (Research Diets, D12450J) for 32 weeks.

Statistical analysis

Data are expressed as mean \pm SEM. Statistical analyses were performed with GraphPad Prism (version 8.0, GraphPad Software, San Diego, CA). Details of the statistical analyses can be found in the supplementary complete materials and methods section.

RESULTS

Ccdc92 was involved in podocyte injury under diabetic conditions In this study, we found that *Ccdc92* was significantly upregulated in the kidneys of *db/db* mice and high-fat diet (HFD)-induced diabetic mice (Fig. 1a, b). Importantly, the expression of *Ccdc92* in glomeruli was positively correlated with the urine albumin-to-creatinine ratio (UACR) (Fig. 1c), suggesting that *CCDC92* might be related to glomerular injury in DKD. Immunofluorescence (IF) staining further showed that *Ccdc92* was expressed in glomerular cells and significantly upregulated in podocytes from diabetic mice (Fig. 1d, Supplementary Fig. S1a), but there was no obvious change of *Ccdc92* expression in endothelial cells or mesangial cells from *db/db* mice (Supplementary Fig. S1b). Moreover, the expression of *Ccdc92* in glomeruli was negatively correlated with the podocyte number in diabetic mice (Fig. 1e, f). In vitro, *Ccdc92* was significantly induced in mouse podocytes exposed to high glucose (HG; Fig. 1g), advanced glycation end products (AGE; Fig. 1h), or cholesterol (Fig. 1i), but there were no obvious changes of *Ccdc92* expression in HG-treated mouse glomerular endothelial cells (MGECs) or mouse mesangial cells (SV40 MES 13) (Fig. 1j, k). Moreover, we further confirmed the upregulation of *Ccdc92* in glomeruli, especially in podocytes, from DKD patients (Fig. 1l, Supplementary Table S1).

Ccdc92 deficiency attenuated podocyte injury in DKD

To better elucidate the role of *Ccdc92* in podocyte injury, mice with podocyte-specific deletion of *Ccdc92* (*Podocin-Cre Ccdc92^{fl/fl}*; *Cre⁺/Ccdc92^{fl/fl}*) were generated by the *Cre-LoxP* recombination system (Supplementary Fig. S2a), which were confirmed by tail

genotyping (Supplementary Fig. S2b), immunofluorescent staining (Supplementary Fig. S2c) and reduction of *Ccdc92* in isolated glomeruli (Supplementary Fig. S2d). All mice were viable and fertile. To establish diabetic mice, *Cre⁺/Ccdc92^{fl/fl}* mice were crossed with *db/+* mice, and the resulting *db/db/Cre⁺/Ccdc92^{fl/fl}* mice and the corresponding control mice were used in this study (Supplementary Fig. S2e). *db/+/Cre⁺/Ccdc92^{fl/fl}* mice did not show any physiological changes, including changes in body weight, kidney weight, heart rate, blood pressure, and glucose level (Supplementary Table S2). However, our results showed that 20-week-old *db/db/Cre⁺/Ccdc92^{fl/fl}* mice exhibited a significant increase in urinary albumin excretion (Fig. 2a), glomerular expansion (Fig. 2b) and podocyte injury (Fig. 2c), as evidenced by glomerular basement membrane (GBM) thickening and podocyte foot process broadening and effacement, which were reversed by podocyte-specific deletion of *Ccdc92* (*db/db/Cre⁺/Ccdc92^{fl/fl}*). We further demonstrated that *Ccdc92* deficiency attenuated podocyte injury in *db/db* mice, based on the upregulation of key podocyte differentiation markers, such as nephrin and podocin (Fig. 2d). Notably, conditional knockout of *Ccdc92* in podocytes significantly reduced podocyte loss in *db/db* mice (Fig. 2e). In addition, we confirmed the detrimental role of *Ccdc92* in HFD-induced diabetic mice and found that podocyte-specific deletion of *Ccdc92* alleviated albuminuria, glomerulosclerosis and podocyte injury (Supplementary Fig. S3a–e, Supplementary Table S2).

In vitro, genetic silencing of *Ccdc92* (Fig. 3a) attenuated actin cytoskeleton disorganization (Fig. 3b) and apoptosis (Fig. 3c, d) and upregulated nephrin and podocin expression (Fig. 3e, f) in podocytes exposed to HG.

Ccdc92 contributed to podocyte lipotoxicity by inhibiting ABCA1-mediated cholesterol efflux

Lipid accumulation was increased in podocytes exposed to HG, based on Nile red staining (Fig. 3g), which was reversed by *Ccdc92* knockdown. In vivo, podocyte-specific deletion of *Ccdc92* reduced the expression of adipophilin, a lipid droplet-specific marker [14], in podocytes from both *db/db* mice (Fig. 3h) and HFD-induced diabetic mice (Supplementary Fig. S3f), suggesting that *Ccdc92* is involved in lipid metabolism of podocyte under DKD.

To explore the role of *CCDC92* in lipid metabolism of podocyte, we performed lipidomic analysis and found that *CCDC92* was mainly involved in cholesterol metabolism pathways in podocytes, according to Kyoto Encyclopedia of Genes and Genomes (KEGG) pathway enrichment analysis of the differentially abundant metabolites

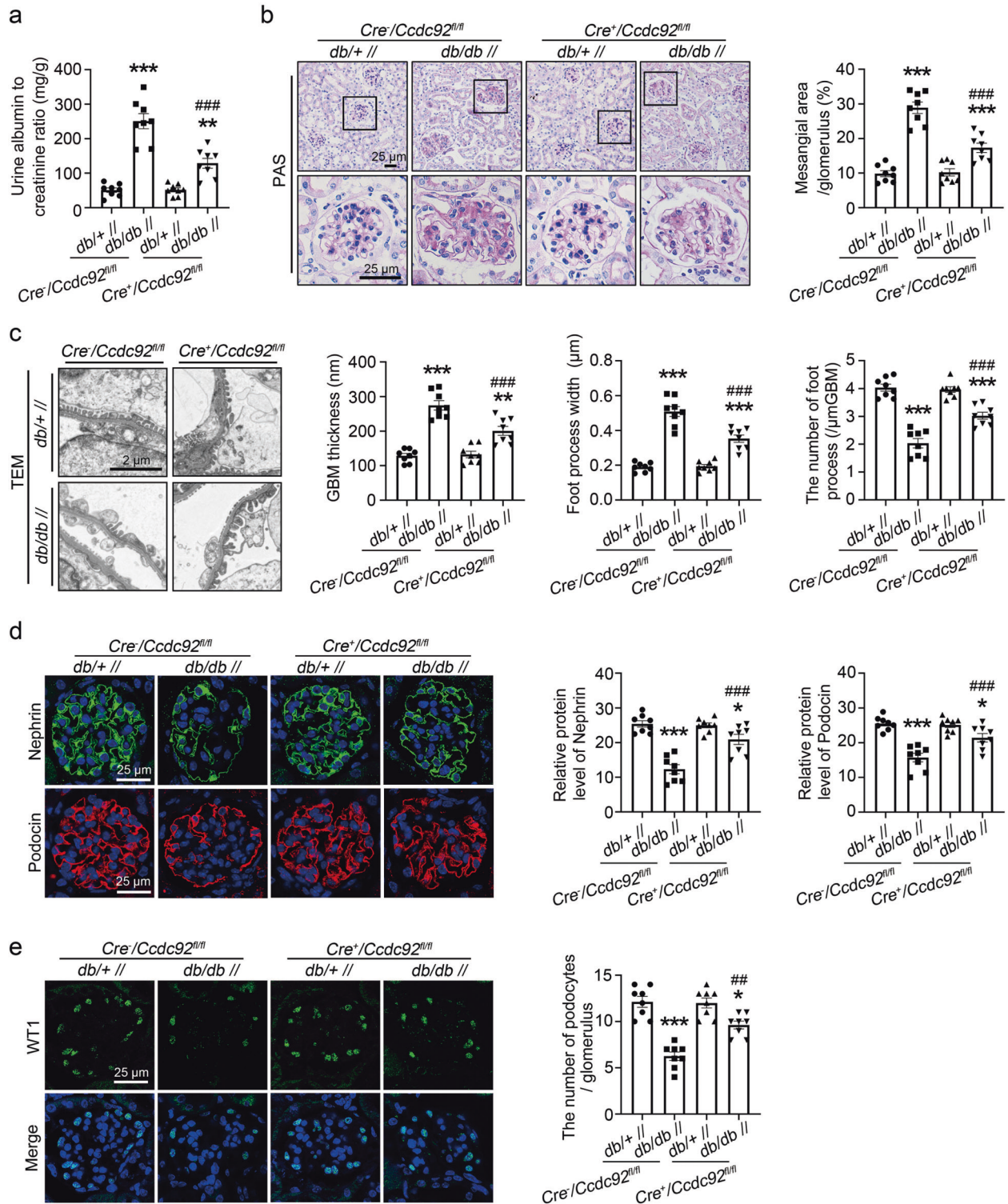


Fig. 2 *Ccdc92* deficiency attenuated podocyte injury in DKD. **a** Urinary albumin creatinine ratio in different groups of mice at 20-week ages ($n = 8$ for each group). $**P < 0.01$, $***P < 0.001$ vs. $db/+//Cre^-/Ccdc92^{fl/fl}$ mice, $###P < 0.001$ vs. $db/db//Cre^-/Ccdc92^{fl/fl}$ mice. **b** Morphological examinations of glomerular changes by periodic acid–schiff (PAS) analyses in mice ($n = 8$ for each group). $***P < 0.001$ vs. $db/+//Cre^-/Ccdc92^{fl/fl}$ mice, $###P < 0.001$ vs. $db/db//Cre^-/Ccdc92^{fl/fl}$ mice. **c** Morphological examinations of glomerular changes by transmission electron microscopy (TEM) analysis in mice ($n = 8$ for each group). $**P < 0.01$, $***P < 0.001$ vs. $db/+//Cre^-/Ccdc92^{fl/fl}$ mice, $###P < 0.001$ vs. $db/db//Cre^-/Ccdc92^{fl/fl}$ mice. **d** Representative immunofluorescence (IF) images showing the expressions of nephrin and podocin in glomeruli from mice ($n = 8$ for each group). $*P < 0.05$, $***P < 0.001$ vs. $db/+//Cre^-/Ccdc92^{fl/fl}$ mice, $###P < 0.001$ vs. $db/db//Cre^-/Ccdc92^{fl/fl}$ mice. **e** Representative IF imaging and quantifications of Wilms' Tumor 1 (WT-1) (green) per glomerulus in the kidney ($n = 8$ for each group). $*P < 0.05$, $***P < 0.001$ vs. $db/+//Cre^-/Ccdc92^{fl/fl}$ mice, $##P < 0.01$ vs. $db/db//Cre^-/Ccdc92^{fl/fl}$ mice. Data are expressed as mean \pm SEM and n indicates the number of biologically independent experiments. Two-way ANOVA followed by Tukey's post-test (**a–e**).

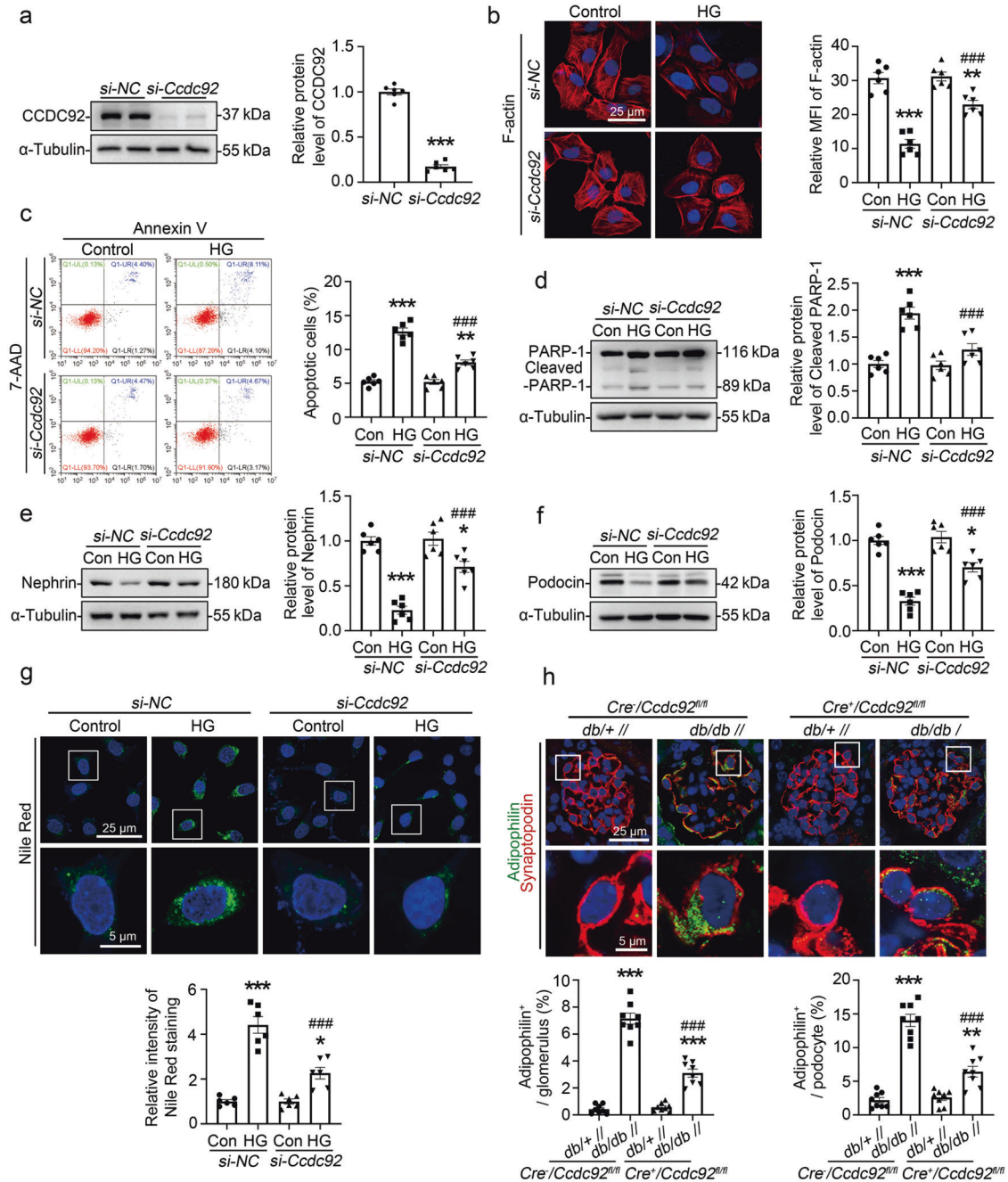


Fig. 3 *Ccdc92* contributed to podocyte lipotoxicity under diabetic conditions. **a** Representative Western blot gel documents and summarized data showing the gene silencing efficiency of *Ccdc92* by a *Ccdc92*-siRNA transfection in podocytes ($n = 6$ for each group). *** $P < 0.001$ vs. scramble (*si-NC*). **b** Representative immunofluorescence (IF) images of F-actin by phalloidine staining ($n = 6$ for each group) in podocytes with different treatments. ** $P < 0.01$, *** $P < 0.001$ vs. scramble (*si-NC*) control, ### $P < 0.001$ vs. scramble of HG treatment. **c** Flow cytometry analysis to evaluate the role of *Ccdc92* on the regulation of apoptosis ($n = 6$ for each group). ** $P < 0.01$, *** $P < 0.001$ vs. scramble (*si-NC*) control, ### $P < 0.001$ vs. scramble of HG treatment. **d** Representative Western blot gel documents and summarized data showing the relative protein levels of cleaved-poly-ADP-ribose polymerase1 (PARP1) in podocytes with different treatments ($n = 6$ for each group). *** $P < 0.001$ vs. scramble (*si-NC*) control, ### $P < 0.001$ vs. scramble of HG treatment. **e** Representative Western blot gel documents and summarized data showing the relative protein levels of nephryn in podocytes with different treatments ($n = 6$ for each group). * $P < 0.05$, *** $P < 0.001$ vs. scramble (*si-NC*) control, ### $P < 0.001$ vs. scramble of HG treatment. **f** Representative Western blot gel documents and summarized data showing the relative protein levels of podocin in podocytes with different treatments ($n = 6$ for each group). * $P < 0.05$, *** $P < 0.001$ vs. scramble (*si-NC*) control, ### $P < 0.001$ vs. scramble of HG treatment. **g** Photomicrographs and quantifications showing Nile Red staining in podocytes from different groups ($n = 6$ for each group). * $P < 0.05$, *** $P < 0.001$ vs. scramble (*si-NC*) control, ### $P < 0.001$ vs. scramble of HG treatment. **h** Representative images and quantifications showing lipid deposition by immunofluorescence staining of adipophilin (green) and synaptopodin (red) in kidney from mice ($n = 8$ for each group). ** $P < 0.01$, *** $P < 0.001$ vs. *db/+* / *Cre*⁺ / *Ccdc92*^{fl/fl} mice, ### $P < 0.001$ vs. *db/db* / *Cre*⁺ / *Ccdc92*^{fl/fl} mice. Data are expressed as mean \pm SEM and n indicates the number of biologically independent experiments. Two-tailed Student's unpaired t test analysis (**a**), Two-way ANOVA followed by Tukey's post-test (**b-h**).

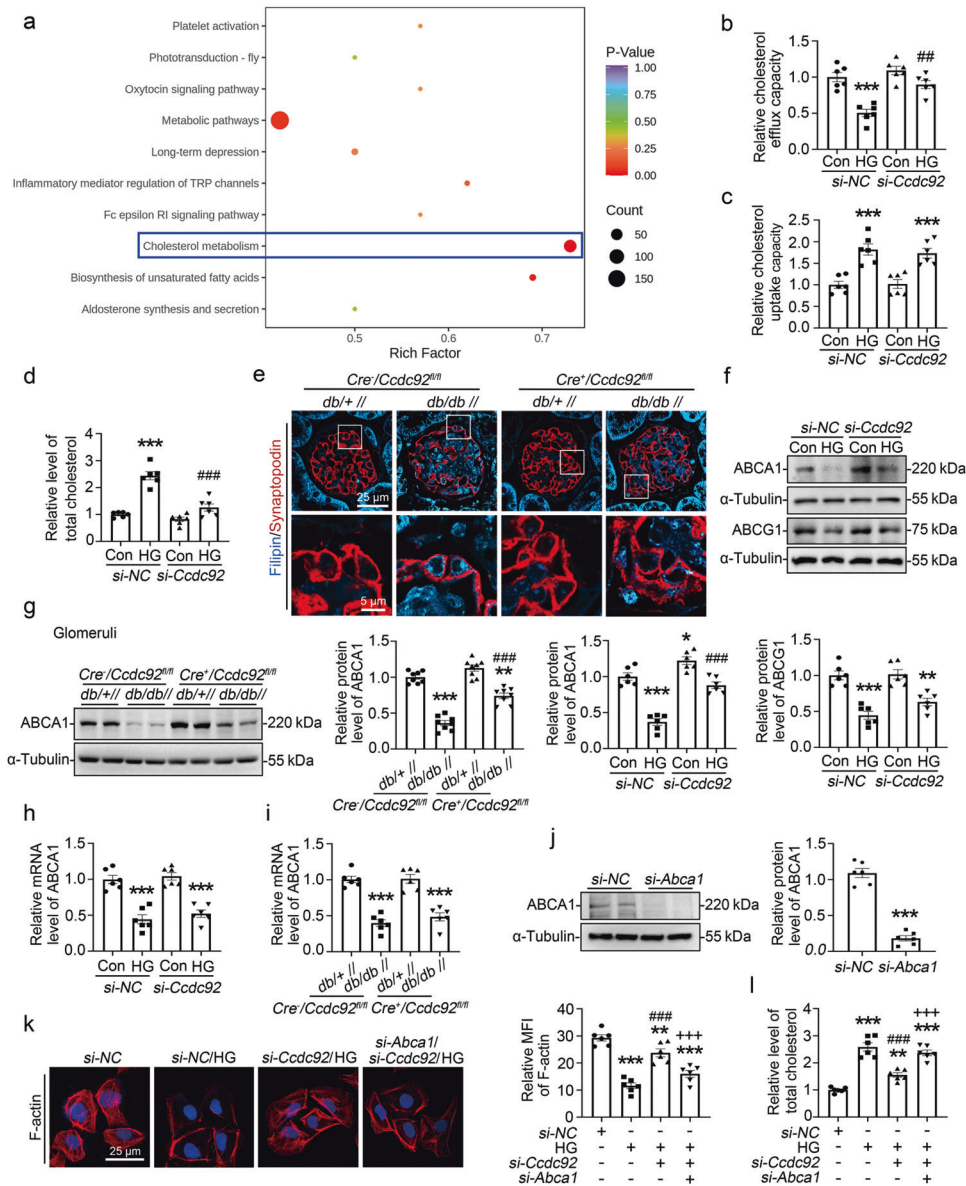


Fig. 4 Ccdc92 contributed to podocyte lipotoxicity by inhibiting ABCA1-mediated cholesterol efflux. **a** Kyoto Encyclopedia of Genes and Genomes (KEGG) pathway enrichment based on the UPLC-MS/MS analysis of podocytes in different groups. Rich factor refers to the ratio of the number of differentially expressed metabolites in the corresponding pathway to the total number of metabolites detected and annotated by the pathway. The size of dots represents the number of differentially significant metabolites enriched in the corresponding pathway. **b** Cholesterol efflux capacity in podocytes with different treatments ($n = 6$ for each group). $***P < 0.001$ vs. scramble (*si-NC*) control, $##P < 0.01$ vs. scramble of HG treatment. **c** Cholesterol uptake in podocytes with different treatments ($n = 6$ for each group). $***P < 0.001$ vs. scramble (*si-NC*) control. **d** Levels of total cholesterol in podocytes with different treatments ($n = 6$ for each group). $***P < 0.001$ vs. scramble (*si-NC*) control, $###P < 0.001$ vs. scramble of HG treatment. **e** Representative images showing cholesterol deposition by immunofluorescence staining of Filipin (blue) and synaptopodin (red) in kidney from mice. **f** Representative Western blot gel documents and summarized data showing the relative protein levels of ABCA1 and ABCG1 in podocytes with different treatments ($n = 6$ for each group). $*P < 0.05$, $**P < 0.01$, $***P < 0.001$ vs. scramble (*si-NC*) control, $###P < 0.001$ vs. scramble of HG treatment. **g** Representative Western blot gel documents and summarized data showing the relative protein levels of ABCA1 in isolated glomeruli from different groups of mice ($n = 8$ for each group). $**P < 0.01$, $***P < 0.001$ vs. *db/+//Cre/Ccdc92^{fl/fl}* mice, $###P < 0.001$ vs. *db/db//Cre/Ccdc92^{fl/fl}* mice. **h** Summarized data showing the effect of Ccdc92 on the mRNA levels of *Abca1* in podocytes treated with HG ($n = 6$ for each group). Levels of the housekeeping gene β -actin were used as an internal control for the normalization of RNA quantity among the samples. $***P < 0.001$ vs. scramble (*si-NC*) control. **i** Summarized data showing the effect of Ccdc92 on the mRNA levels of *Abca1* in isolated glomeruli from different groups of mice ($n = 6$ for each group). Levels of the housekeeping gene β -actin were used as an internal control for the normalization of RNA quantity among the samples. $***P < 0.001$ vs. *db/+//Cre/Ccdc92^{fl/fl}* mice. **j** Representative Western blot gel documents and summarized data showing the gene silencing efficiency of *Abca1* by a *Abca1*-siRNA transfection in podocytes ($n = 6$ for each group). $***P < 0.001$ vs. scramble (*si-NC*). **k** Representative immunofluorescence images of F-actin by phalloidine staining ($n = 6$ for each group) in mouse podocytes with different treatments. $*P < 0.01$, $***P < 0.001$ vs. scramble (*si-NC*) control, $###P < 0.001$ vs. scramble of HG treatment, $+++P < 0.001$ vs. *si-Ccdc92* podocytes with HG. **l** The levels of total cholesterol in podocytes with different treatments ($n = 6$ for each group). $**P < 0.01$, $***P < 0.001$ vs. scramble (*si-NC*) control, $###P < 0.001$ vs. scramble of HG treatment, $+++P < 0.001$ vs. *si-Ccdc92* podocytes (*si-Ccdc92*) with HG. Data are expressed as mean \pm SEM and n indicates the number of biologically independent experiments. Two-tailed Student's unpaired t test analysis (**j**), Two-way ANOVA followed by Tukey's post-test (**b-d**, **f-l**).

Fig. 5 *Ccdc92* deficiency increased the protein level of ABCA1 through the proteasome pathway. **a** Protein–protein interaction (PPI) networks based on Search Tool for the Retrieval of Interacting Genes (STRING) database. The line segment indicates both functional and physical protein associations. **b** Gene Ontology (GO) function analysis in podocytes with or without *Ccdc92* overexpression by Tandem Mass Tags (TMT) proteomics analysis. All differentially expressed proteins are compared with all proteins of the reference species with the annotation results of GO functions, and the significance of the difference between the two is obtained by Fisher's Exact Test. The top abscissa represents the GO secondary functional annotation information, while the bottom represents the statistical results of differential proteins under each GO functional classification. The ordinate represents the percentage of the number of differentially expressed proteins under each functional classification to the total number of differentially expressed proteins. The color represents the significance of the enriched GO functional classification. **c** Proteasome activity represented by the chymotrypsin-like activity in podocytes with different treatments ($n = 6$ for each group). $^*P < 0.05$, $^{**}P < 0.01$, $^{***}P < 0.001$ vs. scramble (*si-NC*) control, $^{###}P < 0.001$ vs. scramble of HG treatment, $^{+++}P < 0.001$ vs. *Ccdc92* knockdown (*si-Ccdc92*) podocytes with HG treatment. **d** Representative Western blot gel documents and summarized data showing the relative protein levels of $\beta 5i$ in isolated glomeruli from different groups of mice ($n = 6$ for each group). $^*P < 0.05$, $^{***}P < 0.001$ vs. *db/+//Cre/Ccdc92^{fl/fl}* mice, $^{###}P < 0.001$ vs. *db/db//Cre/Ccdc92^{fl/fl}* mice. **e** Representative immunofluorescence images of $\beta 5i$ (green) and synaptopodin (red) in glomeruli from different groups of mice. **f** Proteasome activity represented by the chymotrypsin-like activity in podocytes with different treatments ($n = 6$ for each group). $^*P < 0.05$, $^{***}P < 0.001$ vs. scramble (*si-NC*) control, $^{###}P < 0.001$ vs. scramble of HG treatment. **g** Representative Western blot gel documents and summarized data showing the relative protein levels of ABCA1 in podocytes with different treatments ($n = 6$ for each group). $^{***}P < 0.001$ vs. scramble (*OE-NC*) control, $^{##}P < 0.01$ vs. scramble of HG treatment, $^{+++}P < 0.001$ vs. *Ccdc92*-overexpression (*OE-Ccdc92*) podocytes with HG treatment. **h** Representative Western blot gel documents showing the relative levels of Ubiquitin in podocytes with different treatments ($n = 6$ for each group). $^*P < 0.05$, $^{***}P < 0.001$ vs. scramble (*si-NC*) control, $^{###}P < 0.001$ vs. scramble of HG treatment. **i** Representative Western blot gel documents showing the relative levels of Ubiquitin in isolated glomeruli from different groups of mice ($n = 6$ for each group). $^{***}P < 0.001$ vs. *db/+//Cre/Ccdc92^{fl/fl}* mice, $^{\#}P < 0.05$ vs. *db/db//Cre/Ccdc92^{fl/fl}* mice. **j** Representative immunofluorescence images showing the expression of Ubiquitin in podocytes from different groups of mice. Data are expressed as mean \pm SEM and n indicates the number of biologically independent experiments. Two-way ANOVA followed by Tukey's post-test (**c**, **d**, **f**–**i**).

was no obvious change of ABCA1 mRNA level in HG-treated podocytes and isolated glomeruli from diabetic *Cre⁺/Ccdc92^{fl/fl}* mice (Fig. 4h, i), suggesting that a posttranscriptional regulation pathway may be involved in *Ccdc92*-mediated ABCA1 downregulation. In addition, genetic silencing of ABCA1 (Fig. 4j) counteracted the protective role of *Ccdc92* knockdown in podocytes exposed to HG, as evidenced by the increased actin cytoskeleton disorganization (Fig. 4k) and accumulation of total cholesterol (Fig. 4l), indicating that ABCA1 is involved in CCDC92-mediated cholesterol homeostasis in podocytes.

Ccdc92 deficiency increased the protein level of ABCA1 through the proteasome pathway

By analysis based on the Search Tool for the Retrieval of Interacting Genes (STRING), we found that *Ccdc92* interacted with various protease regulatory subunits (Fig. 5a). Moreover, Gene Ontology (GO) analysis (Fig. 5b) in Tandem Mass Tags (TMT) proteomics analysis indicated that *Ccdc92* was related to the regulation of proteasome activity. Therefore, we further assessed the relationship between *Ccdc92* and proteasome activity in podocytes under HG conditions. Our results showed that *Ccdc92* knockdown reduced HG-induced proteasome activity determined by chymotrypsin like activity, which was reversed by overexpression of *Ccdc92* in podocytes (Fig. 5c, Supplementary Fig. S4a). Moreover, podocyte-specific deletion of *Ccdc92* reduced the expression of $\beta 5i$, an immunoproteasome subunit indicating the activation of the ubiquitin–proteasome system (UPS) [16], in isolated glomeruli and podocytes from *db/db* mice (Fig. 5d, e). Furthermore, treatment with MG132, a proteasome inhibitor [17], reduced proteasome activity (Fig. 5f) and increased the protein level of ABCA1 (Fig. 5g), abrogating the effect of *Ccdc92* overexpression on the protein level of ABCA1 in podocytes exposed to HG treatment. Additionally, *Ccdc92* deficiency increased the total level of ubiquitin in HG-treated podocytes and in glomeruli and podocytes from *db/db* mice (Fig. 5h–j). However, genetic silencing of *Ccdc92* did not increase the total level of ubiquitin in MG132-treated podocytes (Supplementary Fig. S4b), suggesting that CCDC92 might regulate the level of ABCA1 through proteasome activity independent of ubiquitination stage.

Ccdc92 promoted HG-induced proteasome activity in podocytes by binding to PA28 α

PA28 α , a well-known and important proteasome activator subunit, plays a crucial role in regulating proteasome activity [18]. Given the properties of the coiled-coil structure of CCDC92 and the

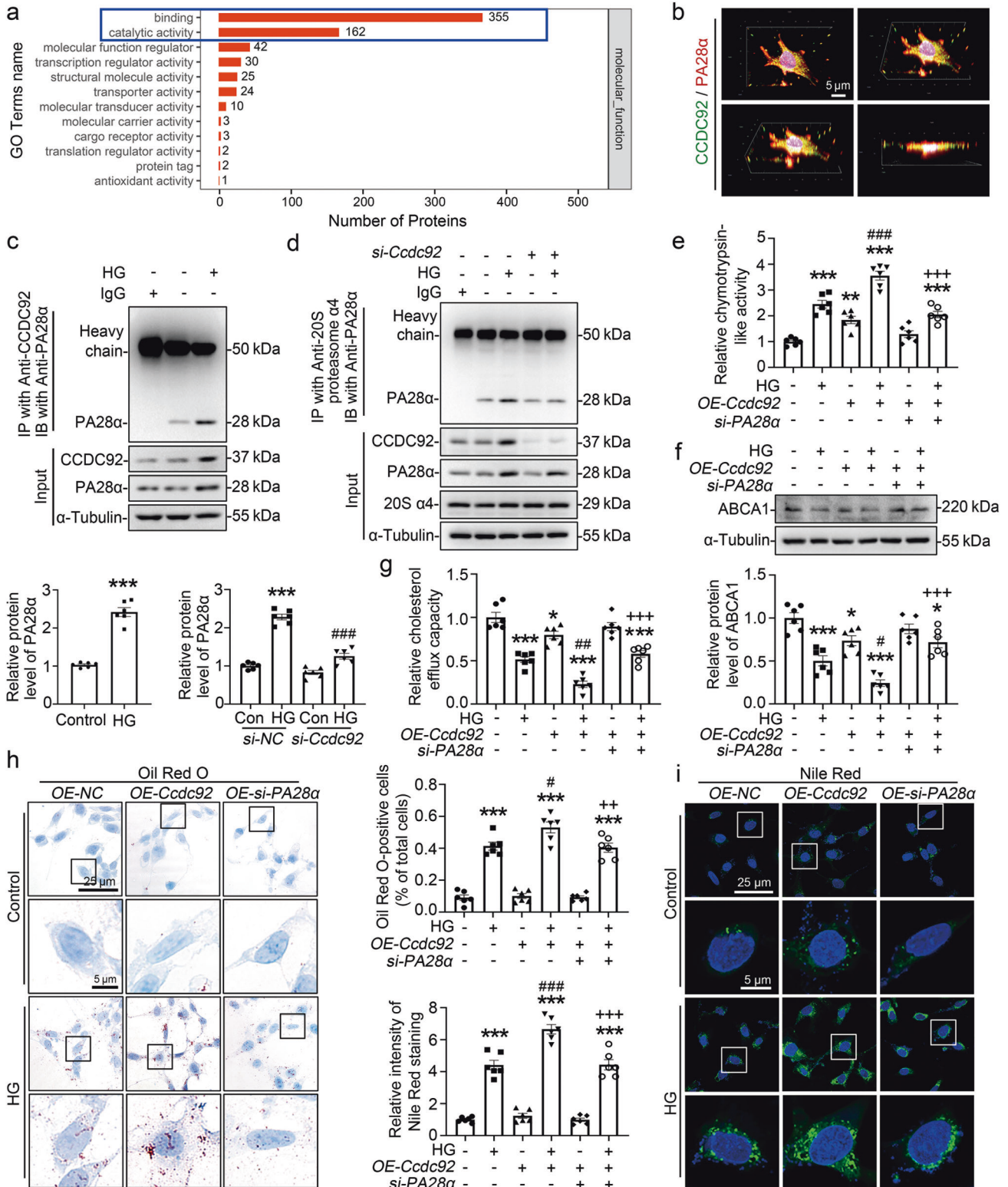
results of STRING and TMT proteomic analyses indicating that the molecular functions of CCDC92 are highly related to “binding” and “catalytic activity” (Fig. 6a), we investigated the interaction between CCDC92 and PA28 α . The results of IF (Fig. 6b) and coimmunoprecipitation (Co-IP) (Fig. 6c) assays confirmed that *Ccdc92* bound to PA28 α and that the binding activity was enhanced under HG conditions (Fig. 6c). It is known that proteasomal degradation is critically dependent on proteasome activators, such as PA28, which bind to the end of the 20 S core particle for reposition of its gating residues and allow access to doomed substrates [19]. Then, we demonstrated by a Co-IP assay that *Ccdc92* deficiency reduced the HG-induced binding between PA28 α and the 20 S core subunit $\alpha 4$ (Fig. 6d). Furthermore, genetic silencing of PA28 α in podocytes (Supplementary Fig. S5a) counteracted the effects of *Ccdc92* on proteasome activation (Fig. 6e), the protein level of ABCA1 (Fig. 6f), the cholesterol efflux capacity (Fig. 6g) and lipid accumulation (Fig. 6h, i). Overexpression of *Ccdc92* aggravated actin cytoskeleton disorganization in podocytes exposed to HG, which was partially reversed by genetic silencing of PA28 α (Supplementary Fig. S5b).

The *Ccdc92* $\Delta 59$ –113 mutation counteracted the effects of *Ccdc92* on podocyte lipotoxicity

Finally, to identify the binding region of CCDC92 to PA28 α , we generated four *Ccdc92* deletion mutants, including two of them lacking aa 1–27 (FLAG-Ccdc92 $\Delta 1$ –27) and aa 59–113 (FLAG-Ccdc92 $\Delta 59$ –113) in the coiled-coil domain predicted by Jpred4 and other two lacking other domains containing aa 153–193 and aa 251–314 (FLAG-Ccdc92 $\Delta 153$ –193, FLAG-Ccdc92 $\Delta 251$ –314) based on the UniProt database (Fig. 7a). It was found that the *Ccdc92* deletion mutant lacking the aa 59–113 in the coiled-coil domain (FLAG-Ccdc92 $\Delta 59$ –113) could not bind to PA28 α , while there were no significant differences in the binding of wild-type (WT) *Ccdc92* and the other three mutants to PA28 α (Fig. 7b). Importantly, our results further confirmed that deletion of aa 59–113 of *Ccdc92* in podocytes abolished the effects of *Ccdc92* on proteasome activation (Fig. 7c), the protein level of ABCA1 (Fig. 7d), the cholesterol efflux capacity (Fig. 7e), lipid accumulation (Fig. 7f, g) and podocyte injury (Supplementary Fig. S6a, b).

DISCUSSION

Although intensive glycemic control or targeting of the renin–angiotensin–aldosterone system (RAAS) with angiotensin-



converting enzyme inhibitors (ACEi) and angiotensin receptor blockers (ARBs) can provide beneficial effects to patients with DKD [20], there is no specific treatment to fully prevent the development of DKD, suggesting that factors other than impaired glucose metabolism and altered hemodynamics can promote DKD. Recently, an increasing number of studies have revealed that

ectopic lipid accumulation, termed lipotoxicity, has been recognized to play a role in the pathogenesis of DKD [2, 21–23]. Among glomerular cells, podocytes are particularly sensitive to lipotoxic injury [3]. It was reported that the accumulation of both cholesterol ester and fatty acid metabolites in podocytes was involved in the pathogenesis of glomerular dysfunction in

Fig. 6 Ccdc92 promoted HG-induced proteasome activity in podocytes by binding to PA28 α . **a** The molecular functions (MF) analysis in podocytes with or without *Ccdc92* overexpression by Tandem Mass Tags (TMT) proteomics analysis. The vertical axis in the figure represents the Gene Ontology (GO) secondary functional annotation information (GO Terms name), and the horizontal axis represents the number of differentially expressed proteins under this functional classification. **b** Representative immunofluorescence images of *Ccdc92* (green) and PA28 α (red) staining in podocytes showing the co-localization. **c** Representative Western blot gel documents and summarized data showing the levels of PA28 α in podocytes with different treatments ($n = 6$ for each group). *Ccdc92* was immunoprecipitated with rabbit antibody to *Ccdc92* and the presence of PA28 α in the immune-complex was assessed by Western blot with the antibody to PA28 α . Negative control using isotype matched normal IgG (rabbit) was done to check for antibody specificity. $***P < 0.001$ vs. control. **d** Representative Western blot gel documents and summarized data showing the levels of PA28 α in podocytes with different treatments ($n = 6$ for each group). The 20 S proteasome $\alpha 4$ was immunoprecipitated with rabbit antibody to 20 S proteasome $\alpha 4$ and the presence of PA28 α in the immune-complex was assessed by Western blot with the antibody to PA28 α . Negative control using isotype matched normal IgG (rabbit) was done to check for antibody specificity. $***P < 0.001$ vs. scramble (*si-NC*) control, $***P < 0.001$ vs. scramble of HG treatment. **e**. Proteasome activity represented by the chymotrypsin-like activity in podocytes with different treatments ($n = 6$ for each group). $**P < 0.01$, $***P < 0.001$ vs. scramble (*OE-NC*) control, $***P < 0.001$ vs. scramble of HG treatment, $+++P < 0.001$ vs. *Ccdc92*-overexpression (*OE-Ccdc92*) podocytes with HG treatment. **f** Representative Western blot gel documents and summarized data showing the relative protein levels of ABCA1 in podocytes with different treatments ($n = 6$ for each group). $*P < 0.05$, $***P < 0.001$ vs. scramble (*OE-NC*) control, $*P < 0.05$ vs. scramble of HG treatment, $+++P < 0.001$ vs. *Ccdc92*-overexpression (*OE-Ccdc92*) podocytes with HG treatment. **g** The cholesterol efflux capacity in podocytes with different treatments ($n = 6$ for each group). $*P < 0.05$, $***P < 0.001$ vs. scramble (*OE-NC*) control, $**P < 0.01$ vs. scramble of HG treatment, $+++P < 0.001$ vs. *Ccdc92*-overexpression (*OE-Ccdc92*) podocytes with HG treatment. **h** Photomicrographs and quantifications showing Oil Red O staining in podocytes from different groups ($n = 6$ for each group). $***P < 0.001$ vs. scramble (*OE-NC*) control, $*P < 0.05$ vs. scramble of HG treatment, $+++P < 0.01$ vs. *Ccdc92*-overexpression (*OE-Ccdc92*) podocytes with HG treatment. **i** Photomicrographs and quantifications showing Nile Red staining in podocytes from different groups ($n = 6$ for each group). $***P < 0.001$ vs. scramble (*OE-NC*) control, $***P < 0.001$ vs. scramble of HG treatment, $+++P < 0.001$ vs. *Ccdc92*-overexpression (*OE-Ccdc92*) podocytes with HG treatment. Data are expressed as mean \pm SEM and n indicates the number of biologically independent experiments. Two-tailed Student's unpaired t test analysis (**c**), Two-way ANOVA followed by Tukey's post-test (**d-i**).

DKD [24]. Notably, cholesterol accumulates in the cytoplasm of podocytes from patients and mice with DKD. Excessive cholesterol accumulation can perturb the slit diaphragm, adversely affect podocyte function and even induce proteinuric kidney diseases [6–8, 25]. However, pharmacological induction of cholesterol efflux with cyclodextrin alleviates podocyte injury in DKD [26], indicating that enhanced cholesterol efflux protects against podocyte injury through reprogramming of cholesterol homeostasis. In this study, we found that upregulation of *Ccdc92* in glomeruli was positively correlated with an increased UACR and podocyte loss in mice with DKD and that *Ccdc92* knockdown significantly increased the cholesterol efflux capacity but had no obvious effect on cholesterol uptake, thereby reducing the total intracellular cholesterol content and attenuating podocyte injury, indicating that CCDC92 might contribute to podocyte lipotoxicity by decreasing cholesterol efflux.

Cholesterol efflux is a sophisticated and dynamic process involving multiple subprocesses and related factors. Among the related factors, ABCA1 and ABCG1 are recognized as the two key factors regulating cholesterol efflux in the context of podocyte injury [7, 8, 27]. In this study, we found that *Ccdc92* preferentially decreased the protein level of ABCA1, which is a transmembrane protein that regulates the efflux of cholesterol and phospholipids in an ATP-dependent manner [28, 29]. ABCA1 expression is positively correlated with the estimated glomerular filtration rate (GFR) [7]. Moreover, podocyte ABCA1 deficiency is sufficient to confer susceptibility to injury in the context of DKD [8], and activation of ABCA1 by its overexpression or by treatment with A30, a pharmacological inducer, ameliorates podocyte injury [8]. In this study, we demonstrated that *Ccdc92* negatively regulated the expression of ABCA1 and that genetic silencing of ABCA1 increased the intracellular cholesterol content in *Ccdc92*-knockdown podocytes exposed to HG, suggesting that CCDC92 might inhibit cholesterol efflux by regulating ABCA1.

Interestingly, we found that *Ccdc92* regulated the protein level rather than the mRNA level of ABCA1 under diabetic conditions, suggesting that this regulation might occur at the posttranscriptional level. The ubiquitin–proteasome system (UPS), one of the major intracellular protein degradation pathways, is important for maintaining cell homeostasis [30]. During this process, upregulation of proteasome activity specifically occurs in patients with membranous nephropathy

(MN), focal segmental glomerulosclerosis (FSGS) and DKD, which is considered as a sign of persistent podocyte injury [31, 32]. Meanwhile, the role of UPS is highlighted in the pathogenesis and progression of various diseases including secondary complications of diabetes, suggesting that targeting the UPS might be a novel strategy to prevent DKD [33]. Importantly, the UPS can also serve as an important determinant for cellular cholesterol homeostasis through the regulation of cholesterol metabolism [34]. Furthermore, proteasomal inhibition can induce the expression of ABCA1 and cholesterol efflux in macrophages [35], suggesting that proteasome regulates cholesterol efflux by mediating ABCA1 expression. The results from our bioinformatics analysis strongly suggested that *Ccdc92* interacted with the proteasome. We further demonstrated that *Ccdc92* regulated the level of ABCA1 via UPS-mediated degradation, consistent with previous studies showing that the ubiquitination degradation pathway contributed to the reduced level of ABCA1 in the context of cell injury [34, 35]. Interestingly, our results showed that genetic silencing of *Ccdc92* did not increase the total level of ubiquitin in MG132-treated podocytes, indicating that CCDC92 might regulate the level of ABCA1 through proteasome activity, independent of ubiquitination stage.

Mechanistically, CCDC92 participates in a variety of biological processes by binding to other proteins [36, 37]. Our proteomic analysis strongly suggested that CCDC92 might interact with some protease subunits with catalytic activity. PA28 α , a well-known and important proteasome activator subunit, is recognized as a key factor in regulating proteasome activity [18]. Moreover, previous studies have reported that the PA28 proteasome and the immunoproteasome are involved in the development of DKD [31]. PA28 α /PA28 β double knockout in mice attenuates albuminuria in the context of DKD [38], suggesting that PA28-mediated alteration of proteasome activity contributes to DKD. Our results demonstrated that *Ccdc92* can bind to PA28 α , consequently enhancing the interaction of PA28 α with the core subunit of the proteasome, in turn promoting proteasome activity and accelerating ABCA1 degradation, finally leading to the disruption of cholesterol homeostasis in podocytes. More accurately, we further found that the aa 59–113 in the coiled-coil domain of *Ccdc92* was necessary for the binding of PA28 α . Moreover, we provided direct evidence for the effects of *Ccdc92* aa59–113 on lipid metabolism

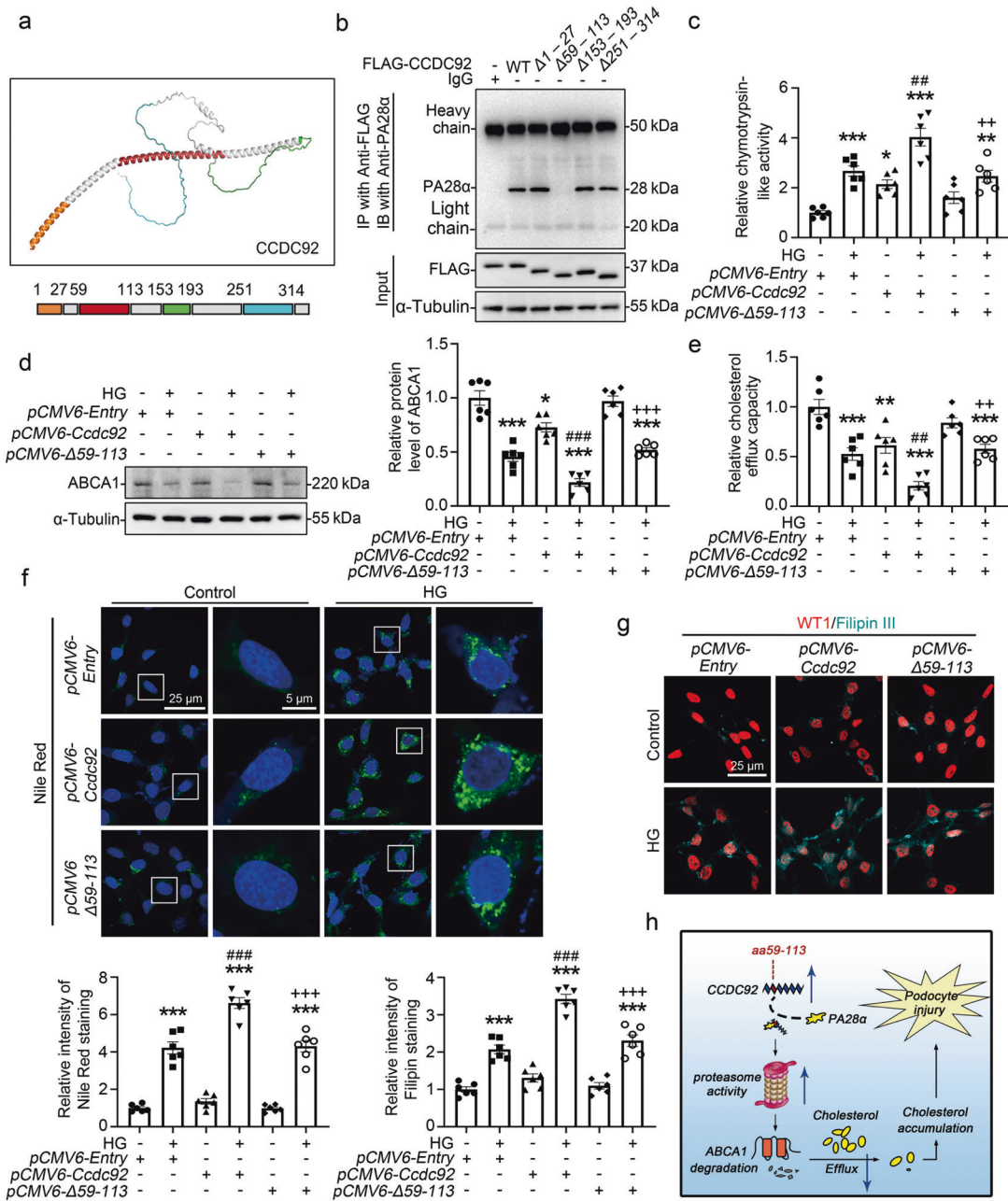


Fig. 7 The Ccdc92 Aaa59-113 mutation counteracted the effects of Ccdc92 on podocyte lipotoxicity. **a** Four different Ccdc92 deletion mutants were constructed, each lacking one of the coiled-coil or other domains predicted by Jpred4 and Uniprot database. **b** Representative Western blot gel documents and summarized data showing the levels of PA28α in podocytes with different treatments. Ccdc92 was immunoprecipitated with the rabbit antibody to FLAG and the presence of PA28α in the immune-complex was assessed by Western blot with the antibody to PA28α. Negative control using isotype matched normal IgG (rabbit) was done to check for antibody specificity. **c** Proteasome activity represented by the chymotrypsin-like activity in podocytes with different treatments ($n = 6$ for each group). $*P < 0.05$, $**P < 0.01$, $***P < 0.001$ vs. control (pCMV6-Entry), $##P < 0.01$ vs. pCMV6-Entry with high glucose (HG) treatment, $+++P < 0.001$ vs. Ccdc92-overexpression podocytes (pCMV6-Ccdc92) with HG treatment. **d** Representative Western blot gel documents and summarized data showing the relative protein levels of ABCA1 in podocytes with different treatments ($n = 6$ for each group). $*P < 0.05$, $***P < 0.001$ vs. pCMV6-Entry, $##P < 0.01$ vs. pCMV6-Entry with HG treatment, $+++P < 0.001$ vs. pCMV6-Ccdc92 with HG treatment. **e** The cholesterol efflux capacity in podocytes with different treatments ($n = 6$ for each group). $**P < 0.01$, $***P < 0.001$ vs. pCMV6-Entry, $##P < 0.01$ vs. pCMV6-Entry with HG treatment, $+++P < 0.001$ vs. pCMV6-Ccdc92 with HG treatment. **f** Photomicrographs and quantifications showing Nile Red staining in podocytes from different groups ($n = 6$ for each group). $***P < 0.001$ vs. pCMV6-Entry, $##P < 0.01$ vs. pCMV6-Entry with HG treatment, $+++P < 0.001$ vs. pCMV6-Ccdc92 with HG treatment. **g** Photomicrographs and quantifications showing cholesterol deposition by immunofluorescence staining of Filipin (green) and Wilms tumor type1 (WT1, red) of podocytes in different groups ($n = 6$ for each group). $***P < 0.001$ vs. pCMV6-Entry, $##P < 0.01$ vs. pCMV6-Entry with HG treatment, $+++P < 0.001$ vs. pCMV6-Ccdc92 with HG treatment. **h** Schematic depicting CCDC92 promotes podocyte injury by regulating PA28α/ABCA1/cholesterol efflux axis in diabetic kidney disease. Data are expressed as mean \pm SEM and n indicates the number of biologically independent experiments. Two-way ANOVA followed by Tukey's post-test (**c-g**).

and podocyte injury, suggesting that the aa 59–113 in the coiled-coil domain of CCDC92 is vital for regulating the PA28 α /ABCA1/cholesterol efflux axis.

Some limitations of this study should be noted. Although we demonstrated that Ccdc92 regulated ABCA1 via the proteasome pathway, we cannot exclude the possibility that other targets of Ccdc92 may also be involved in this process. It is known that the UPS can control all aspects of cholesterol metabolism, including synthesis, uptake and efflux, by regulating specific key molecules, such as ABCG5, ABCG8, liver X receptors (LXRs) α and β , and sterol regulatory element binding proteins (SREBPs) 1 and 2, the master transcriptional regulators of cholesterol metabolism [34], suggesting that the PA28-mediated proteasome system might regulate several molecules related to cholesterol metabolism to promote cholesterol deposition in podocytes. In addition, although recent studies have indicated that Ccdc92 is involved in obesity, T2D and insulin sensitivity [13], few studies have focused on the mechanisms of Ccdc92 in obesity and insulin resistance. In this study, we found that Ccdc92 inhibited cholesterol efflux in podocytes by promoting the degradation of ABCA1, which is also a key factor in regulating adipose tissue lipid content and insulin sensitivity [39]. Therefore, we speculate that similar mechanisms might be involved in these effects of Ccdc92. Further studies are needed to address this possibility.

In conclusion, we demonstrated that Ccdc92 was upregulated in podocytes and promoted lipid accumulation by inhibiting cholesterol efflux. Mechanistically, we found that Ccdc92 promoted the degradation of ABCA1 by regulating PA28 α -mediated proteasome activity (Fig. 7h). Our findings suggest that targeting CCDC92-mediated cholesterol metabolism may constitute a new therapeutic strategy for diabetic kidney disease.

DATA AVAILABILITY

The proteomics data presented in this study are openly available in ProteomeXchange with identifier PXD036050. Other data that support the findings of this study are available from the corresponding author upon reasonable request.

ACKNOWLEDGEMENTS

This study was supported by the National Natural Science Foundation of China (T2321004, 91949202, 82090024, 81873614, 82090021, 81900621, 81970580, 82070753, 82170734, 81800645, 81800643, 22107058); Shandong Provincial Natural Science Foundation, China (ZR2019ZD40, ZR2019MH041, 2023HWYQ-020); The Taishan Scholars Program of Shandong Province, China (tsqn202306074) and Cutting Edge Development Fund of Advanced Medical Research Institute (GGY2023QY01).

AUTHOR CONTRIBUTIONS

FWZ. conducted the in vivo and in vitro experiments, performed data analysis, and helped write the manuscript. ZYL, MWW, JYD, PZD and HRZ. contributed to the experimental design and performed the in vitro experiments. XJW performed the in vivo animal studies. YS and YZ helped design the experiments. JCW performed confocal microscopy. WT and YSX analyzed the data. FY, ZYW, and ML designed the experiments, interpreted the data, wrote the manuscript, and approved the final version of the manuscript for publication.

ADDITIONAL INFORMATION

Supplementary information The online version contains supplementary material available at <https://doi.org/10.1038/s41401-023-01213-4>.

Competing interests: The authors declare no competing interests.

REFERENCES

1. John S. Complication in diabetic nephropathy. *Diabetes Metab Syndr.* 2016;10:247–9.
2. Fu Y, Sun Y, Wang M, Hou Y, Huang W, Zhou D, et al. Elevation of JAML promotes diabetic kidney disease by modulating podocyte lipid metabolism. *Cell Metab.* 2020;32:1052–62.e8.

3. DeFronzo RA, Reeves WB, Awad AS. Pathophysiology of diabetic kidney disease: impact of SGLT2 inhibitors. *Nat Rev Nephrol.* 2021;17:319–34.
4. Wahl P, Ducasa GM, Fornoni A. Nephric and renal lipids in kidney disease development and progression. *Am J Physiol Ren Physiol.* 2016;310:F433–45.
5. Brinkkoetter PT, Bork T, Salou S, Liang W, Mizi A, Ozel C, et al. Anaerobic glycolysis maintains the glomerular filtration barrier independent of mitochondrial metabolism and dynamics. *Cell Rep.* 2019;27:1551–66.e5.
6. Pedigo CE, Ducasa GM, Leclercq F, Sloan A, Mitrofanova A, Hashmi T, et al. Local TNF causes NFATc1-dependent cholesterol-mediated podocyte injury. *J Clin Invest.* 2016;126:3336–50.
7. Herman-Edelstein M, Scherzer P, Tobar A, Levi M, Gafter U. Altered renal lipid metabolism and renal lipid accumulation in human diabetic nephropathy. *J Lipid Res.* 2014;55:561–72.
8. Ducasa GM, Mitrofanova A, Mallela SK, Liu X, Molina J, Sloan A, et al. ATP-binding cassette A1 deficiency causes cardiolipin-driven mitochondrial dysfunction in podocytes. *J Clin Invest.* 2019;129:3387–400.
9. Huang LO, Rauch A, Mazzaferro E, Preuss M, Carobbio S, Bayrak CS, et al. Genome-wide discovery of genetic loci that uncouple excess adiposity from its comorbidities. *Nat Metab.* 2021;3:228–43.
10. Vujkovic M, Keaton JM, Lynch JA, Miller DR, Zhou J, Tcheandjieu C, et al. Discovery of 318 new risk loci for type 2 diabetes and related vascular outcomes among 1.4 million participants in a multi-ancestry meta-analysis. *Nat Genet.* 2020;52:680–91.
11. Zhao W, Rasheed A, Tikkanen E, Lee JJ, Butterworth AS, Howson JMM, et al. Identification of new susceptibility loci for type 2 diabetes and shared etiological pathways with coronary heart disease. *Nat Genet.* 2017;49:1450–7.
12. Klarin D, Zhu QM, Emdin CA, Chaffin M, Horner S, McMillan BJ, et al. Genetic analysis in UK Biobank links insulin resistance and transendothelial migration pathways to coronary artery disease. *Nat Genet.* 2017;49:1392–7.
13. Ren L, Du W, Song D, Lu H, Hamblin MH, Wang C, et al. Genetic ablation of diabetes-associated gene Ccdc92 reduces obesity and insulin resistance in mice. *iScience.* 2023;26:105769.
14. Wang Z, Jiang T, Li J, Proctor G, McManaman JL, Lucia S, et al. Regulation of renal lipid metabolism, lipid accumulation, and glomerulosclerosis in *FVBdb/db* mice with type 2 diabetes. *Diabetes.* 2005;54:2328–35.
15. Fornoni A, Merscher S, Kopp JB. Lipid biology of the podocyte—new perspectives offer new opportunities. *Nat Rev Nephrol.* 2014;10:379–88.
16. Nijholt DA, de Graaf TR, van Haastert ES, Oliveira AO, Berkers CR, Zwart R, et al. Endoplasmic reticulum stress activates autophagy but not the proteasome in neuronal cells: implications for Alzheimer's disease. *Cell Death Differ.* 2011;18:1071–81.
17. Lee DH, Goldberg AL. Proteasome inhibitors: valuable new tools for cell biologists. *Trends Cell Biol.* 1998;8:397–403.
18. Collins GA, Goldberg AL. The logic of the 26 S proteasome. *Cell.* 2017;169:792–806.
19. Lesne J, Locard-Paulet M, Parra J, Zivkovic D, Menneteau T, Bousquet MP, et al. Conformational maps of human 20 S proteasomes reveal PA28- and immunodependent inter-ring crosstalks. *Nat Commun.* 2020;11:6140.
20. Vartak T, Godson C, Brennan E. Therapeutic potential of pro-resolving mediators in diabetic kidney disease. *Adv Drug Deliv Rev.* 2021;178:113965.
21. Kim Y, Lim JH, Kim MY, Kim EN, Yoon HE, Shin SJ, et al. The adiponectin receptor agonist adiporon ameliorates diabetic nephropathy in a model of type 2 diabetes. *J Am Soc Nephrol.* 2018;29:1108–27.
22. Patel M, Wang XX, Magomedova L, John R, Rasheed A, Santamaria H, et al. Liver X receptors preserve renal glomerular integrity under normoglycaemia and in diabetes in mice. *Diabetologia.* 2014;57:435–46.
23. Kang HM, Ahn SH, Choi P, Ko YA, Han SH, Chinga F, et al. Defective fatty acid oxidation in renal tubular epithelial cells has a key role in kidney fibrosis development. *Nat Med.* 2015;21:37–46.
24. Schelling JR. The contribution of lipotoxicity to diabetic kidney disease. *Cells.* 2022;11:3236.
25. Song Y, Liu J, Zhao K, Gao L, Zhao J. Cholesterol-induced toxicity: An integrated view of the role of cholesterol in multiple diseases. *Cell Metab.* 2021;33:1911–25.
26. Merscher-Gomez S, Guzman J, Pedigo CE, Lehto M, Aguillon-Prada R, Mendez A, et al. Cyclodextrin protects podocytes in diabetic kidney disease. *Diabetes.* 2013;62:3817–27.
27. Yang Q, Hu J, Yang Y, Chen Z, Feng J, Zhu Z, et al. Sirt6 deficiency aggravates angiotensin II-induced cholesterol accumulation and injury in podocytes. *Thrombostasis.* 2020;10:7465–79.
28. Wang N, Silver DL, Thiele C, Tall AR. ATP-binding cassette transporter A1 (ABCA1) functions as a cholesterol efflux regulatory protein. *J Biol Chem.* 2001;276:23742–7.
29. Oram JF, Lawn RM. ABCA1. The gatekeeper for eliminating excess tissue cholesterol. *J Lipid Res.* 2001;42:1173–9.
30. Pohl C, Dikic I. Cellular quality control by the ubiquitin-proteasome system and autophagy. *Science.* 2019;366:818–22.

31. Meyer-Schwesinger C. The ubiquitin-proteasome system in kidney physiology and disease. *Nat Rev Nephrol.* 2019;15:393–411.
32. Beeken M, Lindenmeyer MT, Blattner SM, Radon V, Oh J, Meyer TN, et al. Alterations in the ubiquitin proteasome system in persistent but not reversible proteinuric diseases. *J Am Soc Nephrol.* 2014;25:2511–25.
33. Goru SK, Kadakol A, Gaikwad AB. Hidden targets of ubiquitin proteasome system: to prevent diabetic nephropathy. *Pharmacol Res.* 2017;120:170–9.
34. Sharpe LJ, Cook EC, Zelcer N, Brown AJ. The UPS and downs of cholesterol homeostasis. *Trends Biochem Sci.* 2014;39:527–35.
35. Ogura M, Ayaori M, Terao Y, Hisada T, Iizuka M, Takiguchi S, et al. Proteasomal inhibition promotes ATP-binding cassette transporter A1 (ABCA1) and ABCG1 expression and cholesterol efflux from macrophages in vitro and in vivo. *Arterioscler Thromb Vasc Biol.* 2011;31:1980–7.
36. Chaki M, Airik R, Ghosh AK, Giles RH, Chen R, Slaats GG, et al. Exome capture reveals ZNF423 and CEP164 mutations, linking renal ciliopathies to DNA damage response signaling. *Cell.* 2012;150:533–48.
37. Bernatik O, Pejškova P, Vyslouzil D, Hanakova K, Zdrahal Z, Cajanek L. Phosphorylation of multiple proteins involved in ciliogenesis by Tau Tubulin kinase 2. *Mol Biol Cell.* 2020;31:1032–46.
38. Yadranji Aghdam S, Mahmoudpour A. Proteasome activators, PA28alpha and PA28beta, govern development of microvascular injury in diabetic nephropathy and retinopathy. *Int J Nephrol.* 2016;2016:3846573.
39. de Haan W, Bhattacharjee A, Ruddle P, Kang MH, Hayden MR. ABCA1 in adipocytes regulates adipose tissue lipid content, glucose tolerance, and insulin sensitivity. *J Lipid Res.* 2014;55:516–23.

Springer Nature or its licensor (e.g. a society or other partner) holds exclusive rights to this article under a publishing agreement with the author(s) or other rightsholder(s); author self-archiving of the accepted manuscript version of this article is solely governed by the terms of such publishing agreement and applicable law.